European Journal of Medicinal Chemistry 169 (2019) 111–120

Contents lists available at ScienceDirect

European Journal of Medicinal Chemistry

journal homepage: http://www.elsevier.com/locate/ejmech

Research paper

sp^2-Iminosugar glycolipids as inhibitors of lipopolysaccharide-mediated human dendritic cell activation in vitro and of acute inflammation in mice in vivo

Evelyne Schaeffer [a], Elena M. Sánchez-Fernández [b], Rita Gonçalves-Pereira [b], Vincent Flacher [a], Delphine Lamon [a], Monique Duval [a], Jean-Daniel Fauny [a], José M. García Fernández [c], Christopher G. Mueller [a, **], Carmen Ortiz Mellet [b, *]

[a] Université de Strasbourg, CNRS, Immunopathology and Therapeutic Chemistry, UPR 3572, 67000, Strasbourg, France
[b] Department of Organic Chemistry, Faculty of Chemistry, University of Seville, c/ Profesor García González 1, 41012, Seville, Spain
[c] Chemical Research Institute (IIQ), CSIC – University of Seville, Avda. Américo Vespucio 49, E-41092, Seville, Spain

ARTICLE INFO

Article history:
Received 22 January 2019
Received in revised form
28 February 2019
Accepted 28 February 2019
Available online 5 March 2019

Keywords:
Iminosugar
Glycolipid
Inflammation
Dendritic cell
Sulfoxide
Sulfone

ABSTRACT

Glycolipid mimetics consisting of a bicyclic polyhydroxypiperidine-cyclic carbamate core and a pseudoanomeric hydrophobic tail, termed sp^2-iminosugar glycolipids (sp^2-IGLs), target microglia during neuroinflammatory processes. Here we have synthesized and investigated new variants of sp^2-IGLs for their ability to suppress the activation of human monocyte-derived dendritic cells (DCs) by lipopolysaccharide (LPS) signaling through Toll-like receptor 4. We report that the best lead was (1*R*)-1-dodecylsulfonyl-5*N*,6*O*-oxomethylidenenojirimycin (DSO_2-ONJ), able to inhibit LPS-induced TNFα production and maturation of DCs. Immunovisualization experiments, using a mannoside glycolipid conjugate (MGC) that also suppress LPS-mediated DC activation as control, evidenced a distinct mode of action for the sp^2-IGLs: unlike MGCs, DSO_2-ONJ did not elicit internalization of the LPS co-receptor CD14 or induce its co-localization with the Toll-like receptor 4. In a mouse model of LPS-induced acute inflammation, DSO_2-ONJ demonstrated anti-inflammatory activity by inhibiting the production of the pro-inflammatory interleukin-6. The ensemble of the data highlights sp^2-IGLs as a promising new class of molecules against inflammation by interfering in Toll-like receptor intracellular signaling.

1. Introduction

sp^2-Iminosugars are an original family of sugar look-alikes possessing a pseudoamide-type nitrogen atom with a high sp^2-hybridation character at the position of the endocyclic oxygen [1–3], with the unique property of mimicking not only the structure and function of the natural counterparts, as classical iminosugars do, but also their chemistry [4]. Most significantly, sp^2-iminosugars can engage in glycosylation reactions, affording stable glycoconjugate analogs capable of agonizing or antagonizing the biological processes in which the natural counterparts are involved. Examples that illustrate the opportunities that sp^2-iminosugar conjugates offer in biology and medicine are the design of pharmacological chaperones targeting lysosomal glycosidases [5], the synthesis of multivalent constructs to explore multivalent enzyme inhibition [6] or the preparation of Tn antigen glycopeptide mimics [7].

Pursuing our interest in the potential of sp^2-iminosugars as monosaccharide surrogates for neoglycoconjugate drug development, we recently turned our attention to glycolipids as immunoactive agents for clinical and mechanistic applications, a very active research area in medicinal chemistry. Studies report that glycolipids exert antiinflammatory and antiproliferative activity, as well as beneficial effects on lipid metabolism [8]. The chemical synthesis of glycolipid analogs is often challenging, however, especially when it comes to producing pure anomeric forms of the sugar head group. Remarkably, sp^2-iminosugars benefit from an exacerbated anomeric effect, which warrants total α-stereoselectivity during *O*-, *S* or *N*- glycosylation steps and imparts

* Corresponding author.
** Corresponding author.
E-mail addresses: c.mueller@ibmc-cnrs.unistra.fr (C.G. Mueller), mellet@us.es (C. Ortiz Mellet).

https://doi.org/10.1016/j.ejmech.2019.02.078
0223-5234/

chemical and enzymatic stability to the resulting glycosides. Indeed, some sp^2-iminosugar glycolipids (sp^2-IGLs) have been already prepared and found to exhibit a range of bioactivities including anti-proliferative [9], anti-metastatic [10,11], anti-parasitic [12] and anti-neuroinflammatory activity [13,14]. The sp^2-IGL representatives (1*R*,*SR*)1-dodecylsulfinyl-5*N*,6*O*-oxomethylidenenojirimycin (*R*-DSO-ONJ) and (1*R*)-1-dodecylsulfonyl-5*N*,6*O*-oxomethylidenenojirimycin (DSO_2-ONJ) were particularly efficient at inhibiting the lipopolysaccharide (LPS)-induced inflammatory signaling in mouse Bv.2 microglial cells by decreasing inducible nitric oxide synthase (iNOS) and pro-inflammatory cytokine production and simultaneously upregulating production of the anti-inflammatory cytokine IL-10. The latter compound was able to significantly reduce reactive gliosis in retinal explants of the diabetic *db*|*db* mice model that recapitulates the progression of diabetic retinopathy [14,15]. Although initially the protein target was hypothesized to be an endoplasmic reticulum α-glucosidase, the sp^2-IGLs were found not to impact glycoprotein biosynthesis, which is consistent with their lack of toxicity in healthy cells [16]. Instead, they seemed to interfere with the mitogen activated protein kinase (MAPK) cascade, at the crossroad between immunity and cancer, offering new therapeutic opportunities.

Dendritic cells (DCs), present in most tissues and body liquids, are key players in the initiation and polarization of the immune response [17]. The investigation of key indicators of the inflammatory response in DCs upon treatment with sp^2-IGLs was therefore mandatory to validate the above notion. These immune sentinels are highly sensitive to innate immune stimuli and mature into professional antigen-presenting cells producing inflammatory cytokines, such as TNFα, and upregulating the T cell co-stimulators CD83 and CD86 at the cell surface. Mature DCs are highly efficient in priming the T cell-mediated adaptive immune response [17]. A particularly efficient DC stimulator is LPS, an important toxin found in the outer membrane of Gram-negative bacteria involved in the development of septic shock, characterized by the hyperproduction of inflammatory cytokines and organ damage [18]. LPS-elicited acute inflammatory responses are mediated by the signaling receptor Toll-like receptor (TLR)-4. The signaling cascade is activated by the successive interaction of LPS with the lipopolysaccharide binding protein, the cluster differentiation antigen CD14, and the myeloid differentiation protein (MD-2) that binds LPS and presents it in a monomeric form to TLR-4 [19]. TLR-4 undergoes dimerization and recruits downstream adaptor proteins, which initiates an intracellular signaling cascade that leads to nuclear translocation of transcription factors and the biosynthesis of pro-inflammatory cytokines and interferons [20,21]. Therefore, therapeutic interventions to reduce TLR-4 signaling in response to LPS are of clinical importance.

With the objective to gather information on the mode of action of sp^2-IGLs and on the structural features that determine their anti-inflammatory properties, we have now generated a series of derivatives **1**–**8** (Fig. 1) that keep the dodecylsulfinyl or dodecylsulfonyl lipidic aglycone moiety but differ in the hydroxylation pattern (D-*gluco*, D-*galacto* or D-*manno*) of the sp^2-iminosugar aglycone, and studied their capacity to inhibit the activation of human DCs by LPS. The sulfone derivative DSO_2-ONJ (compound **3**), having a hydroxylation profile of structural complementarity to α-D-glucopyranosides, emerged as the most active member in reducing TNFα production and downregulating the DC maturation markers CD83 and CD86. Interestingly, co-localization studies support that sp^2-IGLs act by inhibition of intracellular signaling rather than by modifying LPS receptor cell-surface localization. This behavior is sharply different from that reported for other neoglycolipids such as the mannoside glycolipid conjugate (MGC) **9** (Fig. 1), which suppress TLR-4 signaling in human DCs by targeting

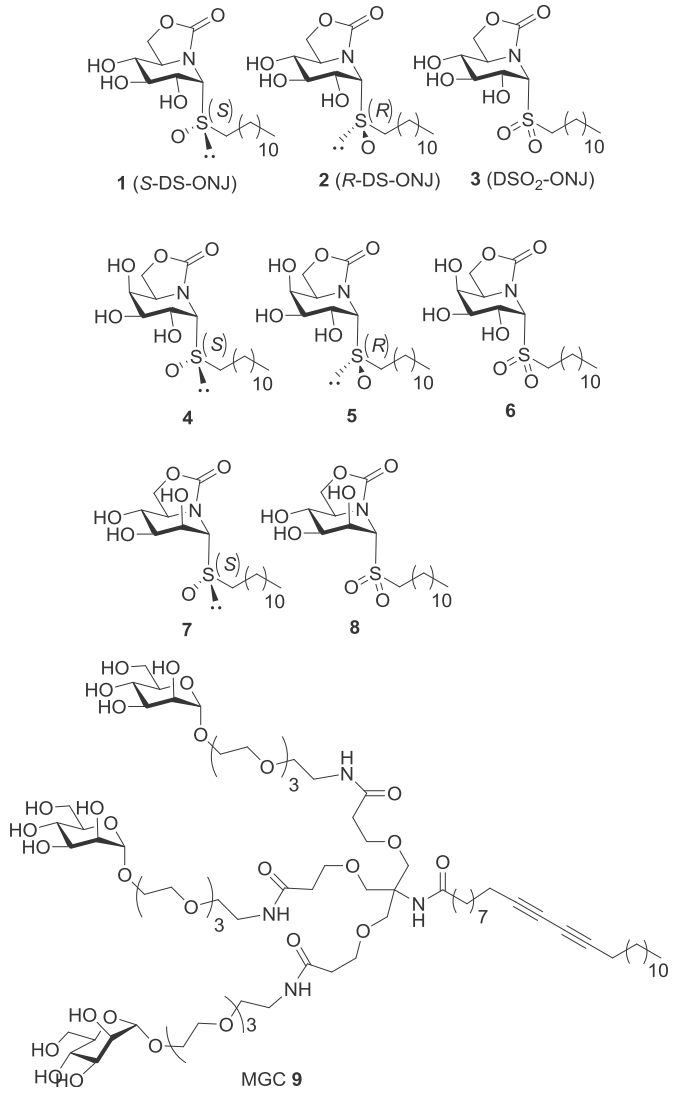

Fig. 1. Structures of sp^2-IGL derivatives (**1**–**8**) and the mannoside glycolipid conjugate (MGC) **9** evaluated in this study.

early membrane steps of the CD14—TLR-4 signaling membrane complex [22–24]. In a mouse model of endotoxin shock, sp^2-IGL **3** reduced the production of the inflammatory interleukin 6 (IL-6), supporting its therapeutic potential.

2. Results

2.1. Design rational and synthesis

Compounds **1**–**8** were chosen for the initial cell toxicity and anti-inflammatory activity-screening, primarily because sp^2-IGLs bearing sulfur anomeric functional groups and twelve-carbon aliphatic aglycones were previously identified as privileged structures in anti-cancer/anti-inflammatory tests in different settings [13,14,16]. The sulfinyl and sulfonyl derivatives, differing in their oxidation state, have been suggested [14] to emulate the phosphate group in anti-inflammatory phosphatidylinositol analogs (PIAs) and alkyl ether lipids (e.g., perifosine) for which a mechanism of action involving p38 MAPK binding has been evidenced [25]. Dodecyl-sulfinyl and -sulfonyl conjugates were therefore considered with sp^2-iminosugar moieties that mimic D-*gluco* (**1**–**3**), D-

galacto (**4**–**6**) and D-*manno* (**7** and **8**) glycolipids in order to assess the effect of the glycone configuration in the anti-inflammatory activity.

Compounds **1**–**3** were prepared following previously reported procedures [12,14]. The chemical syntheses of the new derivatives **4**–**8** follow a general scheme involving (i) steroselective α-*S*-glycosidation of the corresponding peracetylated sp^2-iminosugar (**10** or **14**) with dodecanethiol and (ii) partial or full oxidation of the thioglycoside intermediate (**11** or **15**) with *m*-chloroperbezoic acid (*m*-CPBA) to afford the target sulfoxide and sulfone sp^2-IGLs, respectively (Schemes 1 and 2). In the case of the *galacto*-configured sulfoxides, both the (S_S) and the (R_S) diastereomers **12** and **13** were formed in close to 1:1 ratio and could be separated by column chromatography before deacetylation to give **4** and **5**, respectively. Their absolute stereochemistry was assigned based on their ^{1}H NMR spectra. Notably, the H-5 resonance was deshielded by 0.67 ppm in **12** (δ 4.96 ppm) compared with **13** (δ 4.29 ppm). Literature data on alkyl α-D-glycosyl sulfoxides support then the (S_S) assignment for the first one, where H-5 and the sulfoxide oxygen would be located in close proximity in the more favourable exoanomeric-type conformation, that is, with C-2 in the ring and the exocyclic methylene carbon in anti-disposition [26]. The lower magnetic nonequivalence (Δδ) of the methylene protons vicinal to the chiral sulfur atom (SOCH_2) for **12** (57 Hz) as compared with **5** (81 Hz) is also in agreement with the NMR properties reported in the literature for (S_S) and the (R_S) alkyl α-D-glycosyl sulfoxides, respectively [27]. The partial oxidation of the *manno*-configured thioglycoside **15** afforded a major sulfoxide product (**16**) that was obtained in pure form after column chromatography and assigned the (S_S) configuration based on the Δδ value for the SOCH_2 protons (48 Hz) [27]. The (R_S) diastereomer was detected in the reaction mixture as a trace compound but could not be isolated in pure form. Finally, deacetylation of **16** by treatment with sodium methylate afforded the fully unprotected target sp^2-IGL **7**.

2.2. Toxicity of sp^2-IGLs on DCs

Human monocyte-derived dendritic cells (DCs) were differentiated from monocytes purified from the blood of different donors. The cytotoxicity of the sp^2-IGL derivatives was evaluated by incubation of the individual components **1**–**8** at 25 and 50 μM concentrations for 24 h, followed by exposure to 7-aminoactinomycin D, a DNA-intercalating fluorescent dye that only penetrates the cell upon cell death. As control, DMSO solvent was added. Assays were performed in parallel in the absence and presence of 100 ng mL^{-1} LPS. In its absence, the mean cell viability did not fall below an 80% threshold at 25 μM or a 70% limit at 50 μM upon treatment with the sp^2-IGLs (Fig. 2a and b). However, in the presence of LPS, cell viability was reduced and fell below 70% for compounds **5** and **6** at 50 μM (Fig. 2a and b). DMSO had no significant impact on cell viability irrespective of LPS. To be in a relatively safe window, we settled the dose limit to 50 μM for future experimentation with the sp^2-IGLs.

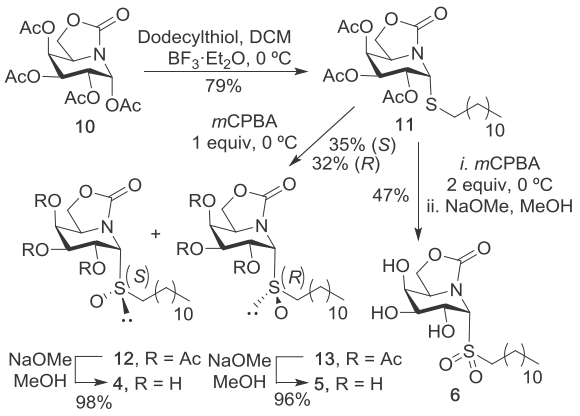

Scheme 1. Synthesis of the D-*galacto*-configured sp^2-IGLs **4**–**6**.

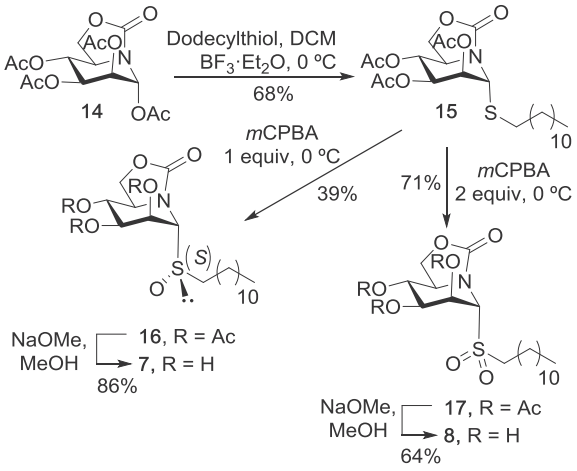

Scheme 2. Synthesis of the D-*manno*-configured sp^2-IGLs **7** and **8**.

2.3. sp^2-IGLs inhibit LPS activation of human DCs

We next examined the capacity of the selected sp^2-IGLs representatives to inhibit the activation of DCs by LPS. By stimulating TLR-4-signaling, LPS is a potent activator of DCs leading to the production of TNFα and the upregulation of the T cell co-stimulators CD83 and CD86. A 24 h exposure time to LPS in the absence or presence of 25 μM and 50 μM of sp^2-IGLs was established to warrant significant expression of endogenous CD83 and CD86 [28,29]. LPS induced the production of TNFα, as determined by ELISA, but there was a significant reduction of TNFα by compound **3** at 25 μM and by compounds **3**–**8** at 50 μM (Fig. 3a and b). The expression of CD83 and CD86 on the cell surface was subsequently assessed by fluorescence-activated flow cytometry (FACS). At 25 μM, compounds **1** and **4** significantly reduced CD83 levels (Fig. 3c). As for CD86, only compound **3** was active at both 25 μM and 50 μM (Fig. 3d). These results showed that most sp^2-IGLs inhibited to some extent LPS-mediated DC maturation, compound **3** being the most active. Subsequent analysis of its TNFα production dose-dependent inhibition on LPS-activated DCs (Fig. 4a) allowed us to establish the dose-response curve for compound 3 and its IC$_{50}$ at 20 ± 10 μM (Fig. 4b). Its efficient downregulatory effect of CD86 expression was also confirmed (Fig. 4c), while there was a significant reduction of CD83 expression only at 50 μM (Fig. 4d). Taken together, the sp^2-IGL **3** displayed a significant anti-LPS activity using human DCs as test cells.

2.4. sp^2-IGL 3 remains active post-LPS exposure

We previously showed that the mannoside glycolipid (MGC) **9** counteracted LPS activation of DCs at similar concentrations as those now encountered for the sp^2-IGL **3** [22]. In order to explore whether or not the two glycolipid mimics behave through similar mechanisms, a direct comparison of compound **3** with MGC **9** for their capacity to antagonize LPS in its stimulatory activity on DCs was conducted. It was observed that MGC **9** impaired TNFα

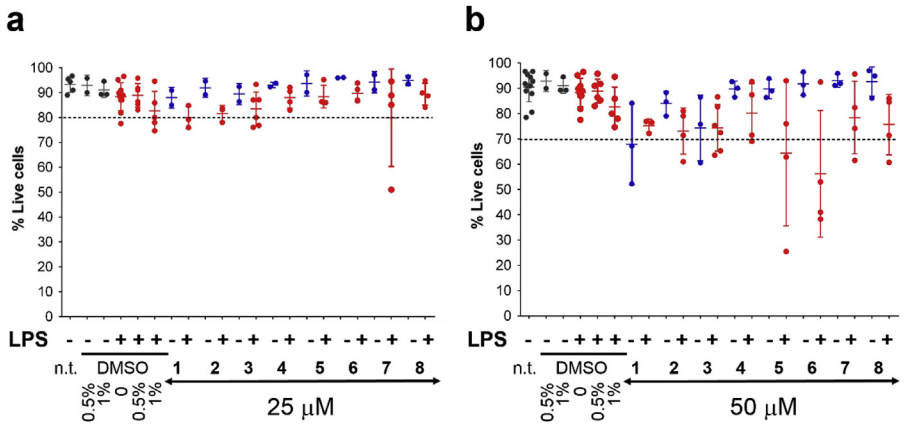

Fig. 2. Effect of sp^2-IGLs on the viability of human DCs. The different sp^2-IGL compounds were used at (a) 25 μM and (b) 50 μM. Solvent controls were performed with DMSO at 0.5 and 1%. Cell viability in the absence or presence of LPS (100 ng mL^{-1}) was measured after 24 h by 7-aminoactinomycin D (7-AAD) staining, followed by flow cytometry analysis. Each point corresponds to a different monocyte blood donor.

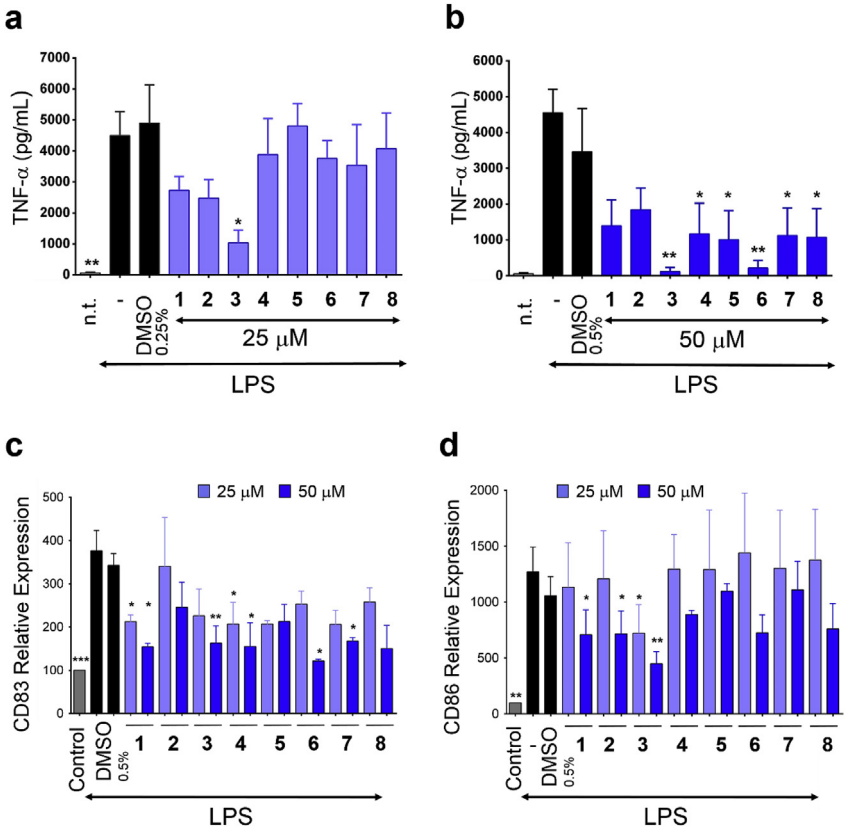

Fig. 3. sp^2-IGLs are anti-inflammatory for LPS-activated DCs. Cells were stimulated with LPS (100 ng mL^{-1}) in the absence or presence of sp^2-IGLs for 24 h (a, 25 μM; b, 50 μM) Effect on the pro-inflammatory cytokine TNF-α released in the media. (c, d) Effect on the relative expression of CD83 and CD86 cell surface maturation markers. Non-treated cells (n.t.; control) or treated with the solvent (DMSO) are indicated. Data correspond to at least 3 cell donors/independent assays. Bars represent means ± SEM.

production more strongly than compound **3** when added at the same time as LPS or 0.5 h after LPS exposure (Fig. 5a and b).

During the first hour of LPS stimulation of macrophages there is an initial delay in the production of biologically active TNFα [30]. This is followed by a rapid increase in TNFα accumulation, reaching a peak by 3 h, followed by a rapid decline, and reaching a plateau in TNFα accumulation in the supernatant by 6 h [31]. Thus, it was of interest to examine sp^2-IGL **3** versus MGC **9** regulation of TNFα production during this time frame. When the compounds were added 2 h, 4 h or 6 h after LPS, it was apparent that while inhibition by compound **3** remained essentially constant, there was a clear loss of MGC **9** activity (Fig. 5a and b). Analysis of CD83 and CD86 markers confirmed these properties (SI, Fig. S1). In summation, MGC **9** was found to be a more potent anti-inflammatory agent when added conjointly with LPS, but compound **3** displayed a more efficient post-LPS inhibitory activity.

2.5. *The mode of operation of sp^2-IGLs and **MGC 9** are different*

The above findings suggest that the mode of action differs

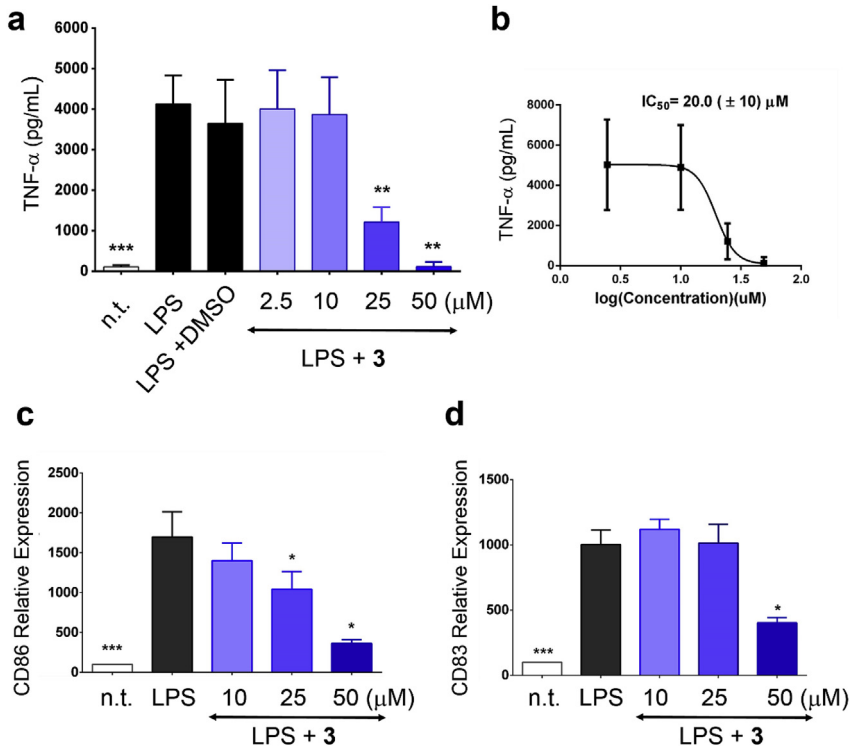

Fig. 4. Anti-inflammatory effects of sp^2-IGL **3** in DCs. Cells were stimulated with LPS (100 ng mL^{-1}) in the absence or presence of **3**, as in Fig. 3. After 24 h, analyses were performed for (a) TNF-α released in the media, (b) IC_{50} on TNF-α production, and (c, d) cell surface maturation markers CD86 and CD83 relative expression. Non-treated cells (n.t.) are indicated. Data correspond to at least 3 cell donors/independent assays. Bars represent means ± SEM.

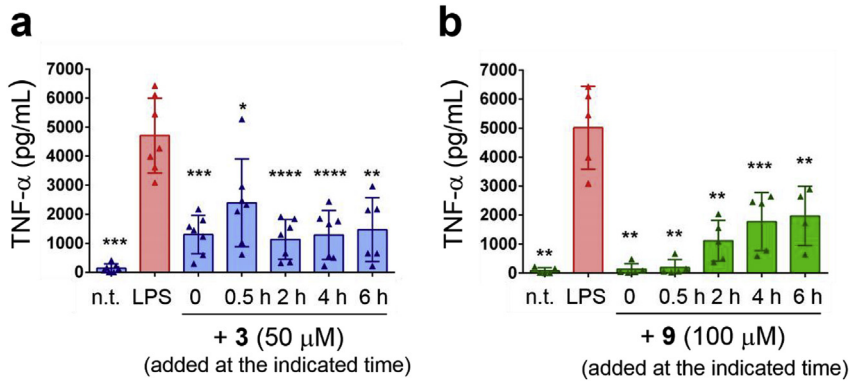

Fig. 5. Delayed addition of compound **3** conserves inhibitory activity. DCs were left untreated (n.t.) or treated with LPS, either alone or with (a) compound **3** or (b) MGC **9**, added at the indicated times. TNF-α production was analyzed after 24 h. Data correspond to the mean (±SD) of n > 3 independent assays (each dot corresponds to an independent assay).

between the MGC and sp^2-IGL LPS-signaling inhibitor families. We have previously shown that MGC **9** at 100 μM elicited CD14 internalization from the cell surface and triggered the co-localization of CD14 with the TLR-4, the two LPS co-receptors, thereby preventing their availability to interact with the LPS at the cell membrane leading to the inflammatory response [22]. To investigate whether sp^2-IGLs affected receptor co-localization, DCs were left untreated or exposed for 30 min to 100 μM of MGC **9** or 25 μM and 50 μM of the D-*gluco*-configured sp^2-IGLs **1**, **2** and **3**, followed by flow cytometry analysis of CD14 cell surface expression. As expected, MGC **9** internalized CD14 from the cell surface, but none of the sp^2-IGLs reduced the CD14 concentration at the cell-surface (Fig. 6a). To assess CD14—TLR-4 co-localization and the potential effect of variations in the monosaccharide mimic configurational pattern, the cells were next labeled with anti-CD14 and anti-TLR-4 antibodies and treated with the more active D-*gluco* compounds, namely the sulfoxide **1** and the sulfone **3**, or the **3**-epimers **6** and **8**, and visualized by confocal microscopy as described.[18] In comparison to untreated cells, MGC **9** provoked the co-localization of the two LPS co-receptors. However, none of the sp^2-IGLs, irrespective of the glycone configuration (**1** and **3** for D-*gluco*, **6** for D-*galacto* and **8** for D-*manno*) induced CD14—TLR-4 proximity (Fig. 6b). These data show that sp^2-IGLs have no impact on cellular LPS-receptor co-localization and support the notion that their inhibitory mechanism is different from that of MGCs.

2.6. *sp^2-Iminosugar glycolipid **3** inhibits acute inflammation in mice*

We next tested if sp^2-IGL **3** can function as an anti-inflammatory

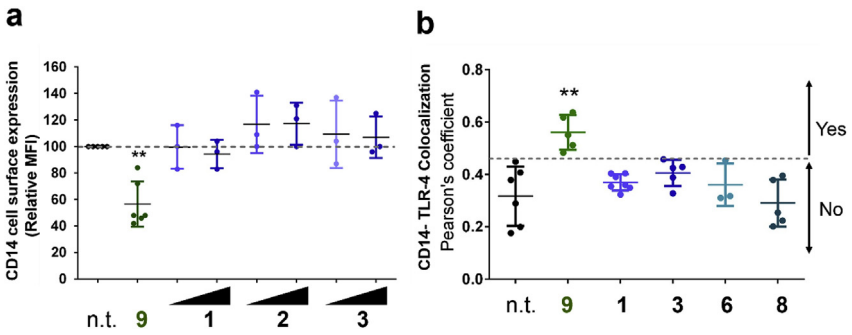

Fig. 6. Effect of sp^2-IGLs on DCs membrane proteins. (a) Cell surface expression of CD14 analyzed by flow cytometry, after 30 min treatment with MGC **9** (100 μM) or compounds **1**, **2**, **3** (25 and 50 μM; light and deep blue dots, respectively). (b) Pearson coefficient of colocalization of CD14 and TLR-4 in permeabilized DCs after 30 min treatment with MGC **9** (100 μM) or compounds **1**, **3**, **6**, **8** (50 μM). Each dot corresponds to a field of 15–20 cells visualized by confocal microscopy. Data correspond to two independent assays. Dots above the grey line (area noted as yes) indicate an increased tendency for colocalization. (For interpretation of the references to colour in this figure legend, the reader is referred to the Web version of this article.)

agent in a mouse model of LPS-induced inflammation. For practical reasons, the response of the proinflammatory interleukin IL-6, which reaches much higher concentrations in serum after LPS administrations as compared with TNFα or other cytokines/chemokines, was determined in this assay [32]. First, toxicity was assessed by comparing the weight change of 2 female and 2 male C57BL/6J mice after repeated intraperitoneal administration of sp^2-IGL **3** or control solvent for 4 successive days. There was no weight loss in either female or male mice, demonstrating good tolerance of the compound at this dose (Fig. 7a and b). Next, mice received intraperitoneally either a single dose of 50 mg/kg of sp^2-IGL **3** or solvent control 1 h prior to a single peritoneal injection of 0.5 mg/kg of LPS. Two hours later, the mice were bled and serum prepared for IL-6 measures by ELISA. As expected [33], the proinflammatory cytokine IL-6 rose to high levels in the blood in response to LPS. However, the administration of sp^2-IGL **3** led to a significant reduction in IL-6 levels. These findings unequivocally show that sp^2-IGL **3** reduces the inflammatory response to LPS stimulation in a mouse model.

3. Discussion

With the aim of exploring alternative therapeutic approaches against inflammation, here we provide a proof-of-principle study, which lays the foundation for novel strategies based on the use of sp^2-iminosugar glycolipids to modulate the intracellular events

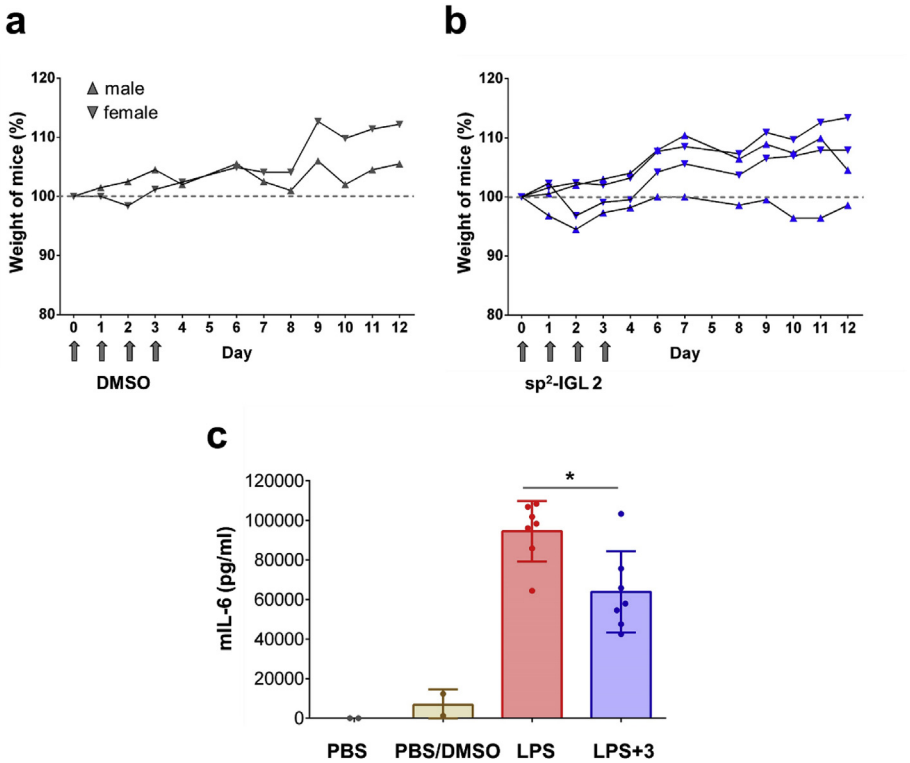

Fig. 7. Compound **3** is active in a mouse model of acute LPS-induced inflammation. (a, b) The weight curves of male and female C57BL/6J mice (relative to their weight on day 0) treated with (a) control PBS/DMSO or (b) compound **3** (30 mg/kg) administered i.p. on day 0, 1, 2, 3, shows the absence of toxic effect of **3**. (c) Mice were treated with solvent (PBS/DMSO 2:1) or compound **3** (in PBS/DMSO; 50 mg/kg) administered i.p., 1 h before LPS (0.5 mg/kg) challenge. Histograms show the IL-6 production in serum 2 h after LPS injection. Bars are mean values ± SD of one typical experiment out of 2. * $p \leq 0.05$.

following an external inflammatory stimulus. The ensemble of data on the expression of LPS-elicited human dendritic cell maturation markers upon treatment with the synthesized sp^2-iminosugar glycolipids evidenced the critical effect of the nature of the functional group linking the glycone portion and the lipid chain in the biological activity. The efficiency of the inflammatory response inhibition is further modulated by the configurational pattern of the sugar-like motif. Thus, sp^2-IGLs with a hydroxylation profile analogous to that of α-D-glucose were more active than the corresponding epimers with α-D-galactose or α-D-mannose configuration. Nevertheless, the changes in the relative orientation of the hydroxyl groups in the sugar-like portion did not affect drastically their potential as anti-inflammatory agents. Sulfone **3** was identified as the most active sp^2-IGL in the series, exhibiting low toxicity *in vitro* up to 50 μM and the capability to inhibit TNFα production in a dose-dependent manner, with an IC_{50} of 20 μM. Time-course addition experiments and determination of the CD14 and the TLR-4 LPS-receptor localization revealed marked differences between the sp^2-IGLs and a control glycolipid, MGC **9**: whereas the latter acts at the cell membrane level, preventing binding of LPS to the CD14 and TLR-4 co-receptors, the sp^2-IGLs do not; therefore, they interfere with TLR-4 intracellular signaling. This is consistent with the reported data suggesting that compound **3** interacts with p38α MAPK in microglia [14]. The promise of small molecule kinase inhibitors for patient benefit in the context of autoimmune and inflammatory processes is well recognized [34]. Finally, our results provide evidence for the efficacy of compound **3** in an *in vivo* model of LPS-mediated inflammation and incite further work on the potential of sp^2-IGLs in anti-inflammatory therapies.

4. Experimental

4.1. General methods

Reagents and solvents were purchased from commercial sources and used without further purification. Optical rotations were measured with a JASCO P-2000 polarimeter, using a sodium lamp (λ = 589 nm) at 22 °C in 1 cm or 1 dm tubes. NMR experiments were performed at 300 (75.5), 400 (100.6) and 500 (125.7) MHz for ^1H (^{13}C, respectively). 2-D COSY and HMQC experiments were carried out to assist on signal assignment. In the FABMS spectra, the primary beam consisted of Xe atoms with maximun energy of 8 keV. The samples were dissolved in *m*-nitrobenzyl alcohol or thioglycerol as the matrices and the positive ions were separated and accelerated over a potential of 7 keV. NaI was added as cationizing agent. For ESI mass spectra, 0.1 pM sample concentrations were used, the mobile phase consisting of 50% aq MeCN at 0.1 mL min^{-1}. Thin-layer chromatography was performed on precoated TLC plates, silica gel 30F-245, with visualization by UV light and by carring with 10% H_2SO_4 or 0.2% w/v cerium (IV) sulphate-5% ammonium molybdate in 2 M H_2SO_4 or 0.1% ninhydrin in EtOH. Column chromatography was performed on Chromagel (silice 60 AC.C 70–200 μm). Deacetylation reactions were carried out by using Zemplén procedure, e.i., addition of NaOMe (0.1 equiv/Ac mol) in MeOH at room temperature, followed by neutralization with solid CO_2, evaporation of the solvent and purification by column chromatography. All compounds were purified to ≥95% purity as determined by elemental microanalysis results obtained on a CHNSTruSpect Micro elemental analyzer (Instituto de Investigaciones Químicas de Sevilla, Spain) from vacuum-dried samples. The analytical results for C, H, N, and S were within ±0.4 of the theoretical values. Compounds **1**–**8** were examined for known classes of assay interference compounds using the freely available research tool for ligand discovery ZINC 15 (http://zinc15.docking.org) [35].[24] Starting materials **10** and **14** [36] and compounds **1**–**3** were synthesized following reported procedures [12]. Mannoside glycolipid conjugate (MGC) **9** was synthesized by the company Roowin (Riom, France). The synthesis, physico-chemical properties and cytotoxicity were previously reported [22–24].

4.2. Synthesis

4.2.1. (1R)-2,3,4-Tri-O-acetyl-1-dodecylthio-5N,6O-oxomethylidenegalactonojirimycin (11)

To a stirred solution of (1*R*)-1,2,3,4-tetra-*O*-acetyl-5*N*,6*O*-oxomethylidenegalactonojirimycin (**10**, 0.29 mmol) in anhydrous DCM (4 mL) at 0 °C, $BF_3.OEt_2$ (134 μL, 1.09 mmol) and dodecylthiol (0.61 mmol) were added under Ar atmosphere. The mixture was stirred for 30 min (TLC monitoring), diluted with DCM (50 mL) and washed with water (10 mL), aq $NaHCO_3$ (10 mL) and brine (10 mL), dried ($MgSO_4$) and concentrated under reduced pressure. Purification by column chromatography (1:3 EtOAc-cyclohexane) yielded **11** (118 mg, 79%). R_f 0.68 (1:1 EtOAc-cyclohexane). $[\alpha]_D$ +161.7 (*c* 1.0 in DCM).^1H NMR (500 MHz, $CDCl_3$): δ 5.78 (d, 1 H, $J_{1,2}$ = 5.1 Hz, H-1), 5.43 (t, 1 H, $J_{3,4} = J_{4,5}$ = 1.6 Hz, H-4), 5.26–5.16 (m, 2 H, H-2, H-3), 4.43–4.34 (m, 2 H, H-5, H-6a), 4.04 (dd, 1 H, $J_{6a,6b}$ = 13.5 Hz, $J_{5,6b}$ = 10.0 Hz, H-6b), 2.57 (ddd, 1 H, $^2J_{H,H}$ = 12.7 Hz, $^3J_{H,H}$ = 8.3 Hz, $^3J_{H,H}$ = 6.0 Hz, SCH_2), 2.43 (ddd, 1 H, SCH_2), 2.17–2.00 (3 s, 9 H, *Me*CO), 1.70–1.20 (m, 20 H, CH_2), 0.87 (t, 3 H, $^3J_{H,H}$ = 7.0 Hz, CH_3).^{13}C NMR (125.7 MHz, $CDCl_3$): δ 170.4–169.8 (Me*CO*), 155.7 (CO), 68.9 (C-3), 68.4 (C-4), 67.2 (C-2), 62.8 (C-6), 58.1 (C-1), 50.4 (C-5), 32.0–22.8 (CH_2), 30.4 (SCH_2), 20.8–20.7 (*Me*CO), 14.2 (CH_3). ESIMS: *m/z* 538.5 $[M + Na]^+$. HRFABMS Calcd for $C_{25}H_{41}NO_8SNa$ $[M + Na]^+$ 538.2451, found 538.2444.

4.2.2. (1R,SS)- and (1R,SR)-2,3,4-Tri-O-acetyl-1-dodecylsulfinyl-5N,6O-oxomethylidenegalactonojirimycin (12 and 13)

To a solution of **11** (131 mg, 0.23 mmol) in DCM (6 mL), *m*CPBA (70%, 40 mg, 0.23 mmol) was added at 0 °C. The reaction mixture was stirred for 10 min, diluted with DCM (50 mL), washed with aqueous $NaHCO_3$ (10 mL), brine (10 mL), dried ($MgSO_4$) and concentrated under reduced pressure. The resulting crude was purified by column chromatography (1:2 EtOAc-cyclohexane) to afford the pure diastereomers **12** and **13**.

Yield of **12**: 44 mg (35%). R_f 0.53 (3:2 EtOAc-cyclohexane). $[\alpha]_D$ +68.4 (*c* 0.8 in DCM). ^1H NMR (300 MHz, $CDCl_3$): δ 5.72 (dd, 1 H, $J_{2,3}$ = 10.7 Hz, $J_{3,4}$ = 2.6 Hz, H-3), 5.49 (t, 1 H, $J_{4,5}$ = 2.6 Hz, H-4), 5.45 (dd, 1 H, $J_{1,2}$ = 7.5 Hz, H-2), 5.05 (d, 1 H, H-1), 4.96 (ddd, 1 H, $J_{5,6a}$ = 9.2 Hz, $J_{5,6b}$ = 3.8 Hz, H-5), 4.50 (t, 1 H, $J_{6a,6b}$ = 9.2 Hz, H-6a), 4.07 (dd, 1 H, H-6b), 2.84 (ddd, 1 H, $^2J_{H,H}$ = 13.0 Hz, $^3J_{H,H}$ = 8.1 Hz, $^3J_{H,H}$ = 6.8 Hz, $SOCH_2$), 2.65 (ddd, 1 H, $SOCH_2$), 2.17–2.01 (2 s, 9 H, MeCO), 1.78–1.20 (m, 20 H, CH_2), 0.87 (t, 3 H, $^3J_{H,H}$ = 6.6 Hz, CH_3). ^{13}C NMR (75.5 MHz, $CDCl_3$): δ 170.3–169.5 (Me*CO*), 157.3 (CO), 68.9–68.7 (C-3, C-4), 67.0–66.8 (C-1, C-2), 63.9 (C-6), 54.2 (C-5), 49.3 ($SOCH_2$), 32.0–22.8 (CH_2), 20.7 (*Me*CO), 14.2 (CH_3). ESIMS: *m/z* 554.3 $[M + Na]^+$. Anal. Calcd for $C_{25}H_{41}NO_9S$: C, 56.48; H, 7.77; N, 2.63; S, 6.03. Found: C, 56.63; H, 7.90; N, 2.44; S, 5.79.

Yield of **13**: 39 mg (32%). R_f 0.47 (3:2 EtOAc-cyclohexane). $[\alpha]_D$ +75.4 (*c* 1.0 in DCM). ^1H NMR (300 MHz, $CDCl_3$): δ 5.65 (dd, 1 H, $J_{2,3}$ = 10.8 Hz, $J_{3,4}$ = 2.6 Hz, H-3), 5.58–5.48 (m, 2 H, H-2, H-4), 5.23 (d, 1 H, $J_{1,2}$ = 6.2 Hz, H-1), 4.42 (t, 1 H, $J_{5,6a} = J_{6a,6b}$ = 9.0 Hz, H-6a), 4.29 (ddd, 1 H, $J_{5,6b}$ = 4.1 Hz, $J_{4,5}$ = 1.6 Hz, H-5), 4.07 (dd, 1 H, H-6b), 2.98 (ddd, 1 H, $^2J_{H,H}$ = 13.0 Hz, $^3J_{H,H}$ = 9.3 Hz, $^3J_{H,H}$ = 5.3 Hz, $SOCH_2$), 2.71 (m, 1 H, $SOCH_2$), 2.18–2.02 (3 s, 9 H, MeCO), 1.90–1.18 (m, 20 H, CH_2), 0.87 (t, 3 H, $^3J_{H,H}$ = 6.6 Hz, CH_3). ^{13}C NMR (75.5 MHz, $CDCl_3$): δ 170.3–169.5 (Me*CO*), 157.3 (CO), 68.9 (C-3), 68.7 (C-4), 67.0 (C-1), 66.8 (C-2), 63.9 (C-6), 52.2 (C-5), 49.3 ($SOCH_2$), 32.0–22.7 (CH_2), 20.7 (*Me*CO), 14.2 (CH_3). ESIMS: *m/z* 554.3 $[M + Na]^+$. Anal. Calcd for $C_{25}H_{41}NO_9S$: C, 56.48; H, 7.77; N, 2.63; S, 6.03. Found: C, 56.55; H, 7.63; N, 2.31; S, 5.67.

4.2.3. (1R,SS)-1-Dodecylsulfinyl-5N,6O-oxomethylidenegalactonojirimycin (4)

Compound **4** was obtained from **12** (30 mg, 0.06 mmol) by conventional *O*-deacetylation (see General Methods) and purification by column chromatography (4:1 EtOAc-cyclohexane → EtOAc). Yield: 24 mg (98%). R_f 0.09 (EtOAc). $[\alpha]_D$ +64.1 (*c* 1.0 in MeOH). ^{1}H NMR (300 MHz, CD_3OD): δ 4.51 (t, 1 H, $J_{6a,6b} = J_{5,6a} = 8.6$ Hz, H-6a), 4.42 (dd, 1 H, $J_{5,6b} = 5.4$ Hz, H-6b), 4.35 (ddd, 1 H, $J_{4,5} = 2.0$ Hz, H-5), 4.29 (dd, 1 H, $J_{2,3} = 9.9$ Hz, $J_{1,2} = 6.8$ Hz, H-2), 3.99 (dd, 1 H, $J_{3,4} = 2.5$ Hz, H-3), 3.88 (t, 1 H, H-4), 3.00–2.82 (m, 2 H, $SOCH_2$), 1.84–1.73 (m, 2 H, $SOCH_2CH_2$), 1.58–1.21 (m, 18 H, CH_2), 0.90 (t, 3 H, $^3J_{H,H} = 6.5$ Hz, CH_3). ^{13}C NMR (75.5 MHz, CD_3OD): δ 160.2 (CO), 72.8–72.4 (C-1, C-3), 70.1 (C-4), 67.7 (C-2), 65.5 (C-6), 57.3 (C-5), 51.9 ($SOCH_2$), 33.0–23.7 (CH_2), 14.4 (CH_3). ESIMS: *m/z* 428.2 $[M + Na]^+$. Anal. Calcd for $C_{19}H_{35}NO_6S$: C, 56.27; H, 8.70; N, 3.45; S, 7.91. Found: C, 56.16; H, 8.65; N, 3.13; S, 7.60.

4.2.4. (1R,SR)-1-Dodecylsulfinyl-5N,6O-oxomethylidenegalactonojirimycin (5)

Compound **5** was obtained from **13** (21 mg, 0.04 mmol) by conventional *O*-deacetylation (see General Methods) and final purification by column chromatography (4:1 EtOAc-cyclohexane → EtOAc). Yield: 15 mg (96%). R_f 0.09 (EtOAc). $[\alpha]_D$ +65.0 (*c* 1.0 in MeOH). ^{1}H NMR (300 MHz, CD_3OD): δ 4.96 (d, 1 H, $J_{1,2} = 6.5$ Hz, H-1), 4.50–4.40 (m, 2 H, H-6a, H-6b), 4.37 (dd, 1 H, $J_{2,3} = 10.0$ Hz, H-2), 4.16 (ddd, 1 H, $J_{5,6a} = 8.7$ Hz, $J_{5,6b} = 5.2$ Hz, $J_{4,5} = 2.0$ Hz, H-5), 4.05 (dd, 1 H, $J_{3,4} = 2.5$ Hz, H-3), 3.90 (t, 1 H, H-4), 3.12 (ddd, 1 H, $^2J_{H,H} = 13.0$ Hz, $^3J_{H,H} = 8.7$ Hz, $^3J_{H,H} = 5.8$ Hz, $SOCH_2$), 2.98 (ddd, 1H, $SOCH_2$), 1.87–1.70 (m, 2 H, $SO_2CH_2CH_2$), 1.60–1.21 (m, 18 H, CH_2), 0.90 (t, 3 H, $^3J_{H,H} = 6.8$ Hz, CH_3). ^{13}C NMR (75.5 MHz, CD_3OD): δ 159.2 (CO), 73.1–72.3 (C-1, C-3), 70.0 (C-4), 69.5 (C-2), 65.3 (C-6), 56.5 (C-5), 50.8 ($SOCH_2$), 33.1–23.7 (CH_2), 14.4 (CH_3). ESIMS: *m/z* 428.2 $[M + Na]^+$. Anal. Calcd for $C_{19}H_{35}NO_6S$: C, 56.27; H, 8.70; N, 3.45; S, 7.91. Found: C, 56.30; H, 8.90; N, 3.17; S, 7.75.

4.2.5. (1R)-1-Dodecylsulfonyl-5N,6O-oxomethylidenegalactonojirimycin (6)

To a solution of **11** (51 mg, 0.09 mmol) in DCM (3 mL), *m*CPBA (70%, 31 mg, 0.18 mmol) was added at 0 °C. The reaction mixture was stirred for 20 min, diluted with DCM (50 mL), washed with aqueous $NaHCO_3$ (10 mL), brine (10 mL), dried ($MgSO_4$), concentrated under reduced pressure. Further purification by column chromatography (4:1 EtOAc-cyclohexane → EtOAc) and conventional *O*-deacetylation (see General Methods) afforded **6**. Yield: 18 mg (47% global yield). R_f 0.20 (EtOAc). $[\alpha]_D$ +23.2 (*c* 1.0 in MeOH). ^{1}H NMR (300 MHz, CD_3OD): δ 5.16 (d, 1 H, $J_{1,2} = 6.0$ Hz, H-1), 4.50 (t, 1 H, $J_{6a,6b} = J_{5,6a} = 8.5$ Hz, H-6a), 4.42 (dd, 1 H, $J_{5,6b} = 5.2$ Hz, H-6b), 4.31 (ddd, 1 H, $J_{4,5} = 1.7$ Hz, H-5), 4.28–4.24 (m, 2 H, H-2, H-3), 3.88 (t, 1 H, $J_{3,4} = 1.7$ Hz, H-4), 3.39–3.34 (m, 2 H, SO_2CH_2), 1.84 (m, 2 H, $^3J_{H,H} = 7.2$ Hz, $SO_2CH_2CH_2$), 1.48–1.29 (m, 18 H, CH_2), 0.90 (t, 3 H, $^3J_{H,H} = 6.7$ Hz, CH_3). ^{13}C NMR (75.5 MHz, CD_3OD): δ 159.2 (CO), 72.3 (C-1), 70.7 (C-2), 70.2 (C-4), 67.8 (C-3), 65.4 (C-6), 56.3 (C-5, CH_2SO_2), 33.0–22.5 (CH_2), 14.4 (CH_3). ESIMS: *m/z* 444.2 $[M + Na]^+$. Anal. Calcd for $C_{19}H_{35}NO_7S$: C, 54.14; H, 8.37; N, 3.32; S, 7.61. Found: C, 53.90; H, 8.18; N, 3.11; S, 7.28.

4.2.6. (1R)-2,3,4-Tri-O-acetyl-1-dodecylthio-5N,6O-oxomethylidenemannonojirimycin (15)

To a stirred solution of (1*R*)-1,2,3,4-tetra-*O*-acetyl-5*N*,6*O*-oxomethylidenemannojirimycin (**14**, 0.29 mmol) in anhydrous DCM (4 mL) at 0 °C, $BF_3.OEt_2$ (134 μL, 1.09 mmol) and dodecylthiol (0.61 mmol) were added under Ar atmosphere. The mixture was stirred for 30 min (TLC monitoring), diluted with DCM (50 mL) and washed with water (10 mL), aq $NaHCO_3$ (10 mL) and brine (10 mL), dried ($MgSO_4$) concentrated under reduced pressure and subjected to column chromatography (1:4 → 1:2 EtOAc-cyclohexane) to give **15**. Yield: 101 mg (68%). R_f 0.72 (1:1 EtOAc-cyclohexane). $[\alpha]_D$ +18.2 (*c* 1.0 in DCM). ^{1}H NMR (300 MHz, $CDCl_3$): δ 5.33–5.28 (m, 2 H, H-2, H-3), 5.22 (t, 1 H, $J_{3,4} = J_{4,5} = 9.9$ Hz, H-4), 5.15 (d, 1 H, $J_{1,2} = 2.0$ Hz, H-1), 4.41 (dd, 1 H, $J_{6a,6b} = 9.1$ Hz, $J_{5,6a} = 8.2$ Hz, H-6a), 4.32 (dd, 1 H, $J_{5,6b} = 5.1$ Hz, H-6b), 4.08 (ddd, 1 H, H-5), 2.73–2.51 (m, 2 H, CH_2S), 2.10–1.99 (3 s, 9 H, MeCO), 1.67–1.51 (m, 2 H, CH_2CH_2S), 1.41–1.17 (m, 18 H, CH_2), 0.86 (t, 3 H, $^3J_{H,H} = 6.6$ Hz, CH_3).^{13}C NMR (75.5 MHz, $CDCl_3$): δ 170.3–169.6 (Me*CO*), 156.3 (CO), 70.8, 69.1 (C-2, C-3), 69.5 (C-4), 66.1 (C-6), 58.3 (C-1), 52.8 (C-5), 31.9–28.7 (CH_2), 20.8–20.6 (*Me*CO), 14.2 (CH_3). ESIMS: *m/z* 538.3 $[M + Na]^+$. Anal. Calcd for $C_{25}H_{41}NO_8S$: C, 58.23; H, 8.01; N, 2.72; S, 6.22. Found: C, 58.32; H, 8.20; N, 2.60; S, 6.04.

4.2.7. (1R,SS)-2,3,4-Tri-O-acetyl-1-dodecylsulfinyl-5N,6O-oxomethylidenemannonojirimycin (16)

To a solution of **15** (131 mg, 0.23 mmol) in DCM (6 mL), *m*CPBA (70%, 40 mg, 0.23 mmol) was added at 0 °C. The reaction mixture was stirred for 10 min, diluted with DCM (50 mL), washed with aqueous $NaHCO_3$ (10 mL), brine (10 mL), dried ($MgSO_4$) and concentrated under reduced pressure. The resulting crude was purified by column chromatography (Et_2O) to give **16**. Yield: 48 mg (39%). R_f 0.59 (Et_2O). $[\alpha]_D$ - 4.1 (*c* 1.0 in DCM). ^{1}H NMR (300 MHz, $CDCl_3$): δ 5.73 (t, 1 H, $J_{1,2} = J_{2,3} = 2.5$ Hz, H-2), 5.61 (dd, 1 H, $J_{3,4} = 9.0$ Hz, H-3), 5.27 (t, 1 H, $J_{4,5} = 9.0$ Hz, H-4), 4.62 (d, 1 H, H-1), 4.60–4.50 (m, 1 H, H-5), 4.52 (t, 1 H, $J_{6a,6b} = J_{5,6a} = 8.3$ Hz, H-6a), 4.38 (dd, 1 H, $J_{5,6b} = 3.7$ Hz, H-6b), 2.95 (m, 1 H, $SOCH_2$), 2.79 (m, 1 H, $SOCH_2$), 2.16–2.01 (3 s, 9 H, MeCO), 1.79–1.18 (m, 20 H, CH_2), 0.87 (t, 3 H, $^3J_{H,H} = 6.9$ Hz, CH_3). ^{13}C NMR (75.5 MHz, $CDCl_3$): δ 170.3–169.4 (Me*CO*), 157.7 (CO), 69.6 (C-2), 69.0 (C-3), 68.8 (C-4), 68.4 (C-1), 66.9 (C-6), 55.8 (C-5), 50.8 ($SOCH_2$), 31.9–22.4 (CH_2), 20.7–20.6 (*Me*CO), 14.1 (CH_3). ESIMS: *m/z* 554.5 $[M + Na]^+$. Anal. Calcd for $C_{25}H_{41}NO_9S$: C, 56.48; H, 7.77; N, 2.63; S, 6.03. Found: C, 56.13; H, 7.44; N, 2.29; S, 5.76.

4.2.8. (1R,SS)-1-Dodecylsulfinyl-5N,6O-oxomethylidenemannonojirimycin (7)

Compound **7** was obtained from **16** (20 mg, 0.04 mmol) by conventional *O*-deacetylation. Column chromatography (5:1 EtOAc-MeOH). Yield: 14 mg (86%). R_f 0.52 (5:1 EtOAc-MeOH). $[\alpha]_D$ +23.8 (*c* 0.6 in MeOH). ^{1}H NMR (300 MHz, CD_3OD): δ 4.67 (d, 1 H, $J_{1,2} = 2.0$ Hz, H-1), 4.63 (t, 1 H, $J_{6a,6b} = J_{5,6a} = 8.7$ Hz, H-6a), 4.38 (t, 1 H, $J_{2,3} = 2.0$ Hz, H-2), 4.34 (dd, 1 H, $J_{5,6b} = 4.9$ Hz, H-6b), 4.11 (ddd, 1 H, $J_{4,5} = 9.3$ Hz, H-5), 3.90 (dd, 1 H, $J_{2,3} = 2.0$ Hz, $J_{3,4} = 9.3$ Hz, H-3), 3.75 (t, 1 H, H-4), 2.98–2.81 (m, 2 H, $SOCH_2$), 1.82–1.71 (m, 2 H, $SOCH_2CH_2$), 1.52–1.24 (m, 18 H, CH_2), 0.90 (t, 3 H, $^3J_{H,H} = 6.7$ Hz, CH_3). ^{13}C NMR (75.5 MHz, CD_3OD): δ 160.5 (CO), 73.6–73.0 (C-1, C-3), 71.9–71.2 (C-2, C-4), 68.7 (C-6), 58.9 (C-5), 51.1 ($SOCH_2$), 33.1–23.6 (CH_2), 14.5 (CH_3). ESIMS: *m/z* 428.3 $[M + Na]^+$. HRFABMS Calcd for $C_{19}H_{35}NO_6SNa$ $[M + Na]^+$ 428.2077, found 428.2081.

4.2.9. (1R)-2,3,4-Tri-O-acetyl-1-dodecylsulfonyl-5N,6O-oxomethylidenemannojirimycin (17)

To a solution of **15** (51 mg, 0.09 mmol) in DCM (3 mL), *m*CPBA (70%, 31 mg, 0.18 mmol) was added at 0 °C. The reaction mixture was stirred for 20 min, diluted with DCM (50 mL), washed with aqueous $NaHCO_3$ (10 mL), brine (10 mL), dried ($MgSO_4$) and concentrated under reduced pressure. Final purification by column chromatography (1:3 EtOAc-cyclohexane) afforded **17**. Yield: 33 mg (71%). R_f 0.66 (1:1 EtOAc-cyclohexane). $[\alpha]_D$ −6.5 (*c* 1.0 in DCM). ^{1}H NMR (300 MHz, $CDCl_3$): δ 5.93 (t, 1 H, $J_{1,2} = J_{2,3} = 2.6$ Hz, H-2), 5.54 (dd, 1 H, $J_{3,4} = 9.0$ Hz, H-3), 5.21 (t, 1 H, $J_{4,5} = 9.0$ Hz, H-4), 5.06 (d, 1 H, H-1), 4.56–4.49 (m, 1 H, H-6a), 4.43–4.37 (m, 2 H, H-5, H-6b), 3.05 (m, 2 H, SO_2CH_2), 2.13–2.02 (3 s, 9 H, MeCO), 1.95–1.78 (m, 2 H, $SO_2CH_2CH_2$), 1.46–1.19 (m, 18 H, CH_2), 0.87 (t, 3 H, $^3J_{H,H} = 6.7$ Hz,

CH_3). ^{13}C NMR (75.5 MHz, $CDCl_3$): δ 170.4–169.2 (Me*CO*), 156.6 (CO), 69.4 (C-1), 69.0 (C-4), 68.9 (C-3), 67.2 (C-6), 65.0 (C-2), 54.1 (C-5), 52.2 (CH_2SO_2), 32.0–21.7 (CH_2), 20.8–20.6 (*Me*CO), 14.2 (CH_3). ESIMS: *m/z* 570.4 $[M + Na]^+$. Anal. Calcd for $C_{25}H_{41}NO_{10}S$: C, 54.83; H, 7.55; N, 2.56; S, 5.85. Found: C, 55.01; H, 7.69; N, 2.29; S, 5.62.

4.2.10. (1R)-1-Dodecylsulfonyl-5N,6O-oxomethylidenemannonojirimycin (8)

Compound **8** was obtained by conventional *O*-deacetylation (see General Methods) of **17**. Column chromatography (4:1 EtOAc-cyclohexane → EtOAc). Yield: 12 mg (64%). R_f 0.20 (EtOAc). $[\alpha]_D$ +23.2 (*c* 1.0 in MeOH). ^1H NMR (300 MHz, CD_3OD): δ 5.03 (d, 1 H, $J_{1,2} = 1.6$ Hz, H-1), 4.65–4.59 (m, 2 H, H-2, H-6a), 4.36 (dd, 1 H, $J_{6a,6b} = 9.0$ Hz, $J_{5,6b} = 5.0$ Hz, H-6b), 4.08 (td, 1 H, $J_{4,5} = J_{5,6a} = 9.0$ Hz, H-5), 3.86 (dd, 1 H, $J_{3,4} = 9.5$ Hz, $J_{2,3} = 3.1$ Hz, H-3), 3.73 (t, 1 H, H-4), 3.25–3.06 (m, 2 H, SO_2CH_2), 1.89–1.73 (m, 2 H, $SO_2CH_2CH_2$), 1.47–1.26 (m, 18 H, CH_2), 0.89 (t, 3 H, $^3J_{H,H} = 6.7$ Hz, CH_3). ^{13}C NMR (75.5 MHz, CD_3OD): δ 159.5 (CO), 74.0 (C-1), 73.0 (C-3), 70.7 (C-4), 68.6 (C-6), 66.9 (C-2), 57.0 (C-5), 52.0 (CH_2SO_2), 32.0–22.7 (CH_2), 14.4 (CH_3). ESIMS: *m/z* 444.3 $[M + Na]^+$. Anal. Calcd for $C_{19}H_{35}NO_7S$: C, 54.14; H, 8.37; N, 3.32; S, 7.61. Found: C, 53.88; H, 8.12; N, 3.04; S, 7.32.

4.3. Cell culture

Human primary cells were cultured at 37 °C and 5% CO_2 in RPMI 1640 supplemented with gentamycin and 10% (v/v) heat-inactivated fetal calf serum (complete medium). Human monocytes were purified from buffy coats by successive Ficoll and Percoll gradients. Monocyte-derived DCs were differentiated from monocytes by 5 days of culture with GM-CSF (50 ng ml^{-1}; ImmunoTools) and IL-4 (10 ng ml^{-1}; ImmunoTools), as described.[19] Proper differentiation was characterized by low CD14 and high CD1a and DC-SIGN expression levels.

4.4. Flow cytometry

The cell phenotype was analyzed using the following antibodies from BD Bioscience: HLA-DR-FITC (Tü39 or L243), DC-SIGN/CD209-PerCP-Cy5.5 (DCN46), CD1a-APC (HI149), CD86-FITC (FUN-1), CD83-APC (HB15e), and CD14-PE (MEM-15, ImmunoTools). Data were acquired on a FACSCalibur (Becton-Dickinson) or Gallios (Beckman-Coulter) after exclusion of dead cells by Sytox Red (Molecular Probes, Invitrogen) or 7-AAD (BD-Pharmingen) DNA intercalating dyes. Data were analyzed using the Cell Quest Pro software (BD Bioscience) or FlowJo (Treestar).

4.5. Cell activation

DCs (10^5 cells/well) were cultured in complete medium (200 μL) and incubated in the presence of Ultra pure E. *coli* K12 lipopolysaccharide (LPS; 100 ng mL^{-1}). Compounds were usually added at the same time as LPS, or, where indicated, 2, 4 or 6 h after LPS addition.

4.6. Enzyme-linked ImmunoabSorbent Assay (ELISA)

After 24 h of stimulation with LPS, cell supernatants were collected and stored at −20 °C. Levels of TNF-α released in the media, or in the case of *in vivo* assays, levels of IL-6 in the mouse sera, were measured by ELISA with the corresponding BD OptEIA Set (BD-Pharmingen).

4.7. Effect on cell surface proteins

DCs (10^5 cells) in complete medium (200 μL) were plated in a 96-well plate. They were left untreated or treated with sp^2-IGLs (25 and 50 μM) or conjugate MGC **9** (100 μM) for 30 min at 37 °C. They were washed, kept on ice, labeled with anti-CD14-PE, and analyzed by flow cytometry.

4.8. Co-localization analysis of CD14 and TLR-4 by confocal microscopy

Assays were performed according to the previously described procedure [22]. Briefly, DCs (10^5 cells per chamber) were cultured on poly-L-Lysine-coated, 8-chambers slides (Lab-Tek, Nunc) in complete medium (300 μL). Cells were left untreated or treated with sp^2-IGLs (50 μM) or MGC **9** (100 μM) for 30 min. Cells were washed, fixed, permeabilized and labeled with anti-TLR-4 polyclonal goat antibody (R&D Systems AF1478, 5 μg mL^{-1}) followed by AF_{488}-donkey anti-goat (Molecular Probes, Invitrogen), and anti-CD14-APC (ImmunoTools). DAPI was used as nuclear counterstaining. Slides were mounted using Fluoromount (Dako). Images were acquired on a Zeiss LSM 780 confocal microscope with GaAsP detector and Zen acquisition software. Images were processed using the ImageJ software.

4.9. In vivo assays in C57BL/6J mice

All animals received humane care in compliance with the guidelines formulated by the French Ministry of Agriculture and of Higher Education and Research, and all procedures were reviewed by the Regional Ethical Committee for Animal Experimentation of the University of Strasbourg. sp^2-IGL **3** was prepared in sterile solvent (7.25 mg mL^{-1}) by solubilization in DMSO (10.5 mg in 1 mL) followed by addition of H_2O (0.5 mL) and PBS x10 (150 μL). LPS (0.5 mg/kg; strain O111.B4; Sigma-Aldrich) was prepared in sterile PBS. To evaluate the *in vivo* toxicity of the compound, 8-week old male and female mice received intraperitoneal (i.p.) administrations of 200 μl of sp^2-IGL **3** (30 mg/kg) or of control DMSO/PBS on day 0, 1, 2, 3. Evaluation of their well-being and weight were performed every day up to day 12. To assess the compounds for their capacity to block LPS-induced IL-6 production, C57BL/6J male 8-week old mice received a single intraperitoneal (i.p.) administration of sp^2-IGL **3** (50 mg/kg) 1 h before LPS (0.5 mg/kg) challenge. Control animals received equivalent volumes of solvent (PBS or PBS/DMSO 2:1) (200 μL) by the intraperitoneal route. Blood (150 μL) was taken 2 h after LPS injection. Serum was prepared and IL-6 measured by ELISA (see above).

Statistical Analysis. Statistical analysis was performed using paired Student's t-test. Data were considered significantly different when p was less than 0.05.

Notes

The authors declare no competing financial interest.

Abbreviations used

DC, dendritic cell; DMSO, dimethyl sulfoxide; DCM, dichloromethane; *m*CPBA, *m*-chloroperoxybenzoic acid; sp^2-IGL, sp^2-iminosugar glycolipid; *R*-DSO-ONJ, (1*R*)-1-dodecylsulfinyl-5*N*,6*O*-oxomethylidenenojirimycin; DSO_2-ONJ, (1*R*)-1-dodecylsulfonyl-5*N*,6*O*-oxomethylidenenojirimycin; LPS, lipopolysaccharide; MGC, mannoside glycolipid conjugate; IL-10, interleukin-10; IL-6, interleukin-6; TNF-α, Tumor Necrosis Factor-α. MAPK, mitogen activated protein kinase.

Acknowledgements

This work was supported by the Centre National de la Recherche Scientifique and the Agence Nationale pour la Recherche (Program "Investissements d'Avenir", ANR-10-LABX-0034 MEDALIS; ANR-11-EQPX-022). This work was also supported by grants from the Spanish Ministry of Economy and Competitiveness: SAF2016-76083-R (MINECO-FEDER) and CTQ2015-64425-C2-1-R (MINECO-FEDER). We thank the Strasbourg/Esplanade imaging platform. Technical assistance from the research support services of the University of Seville (CITIUS) is also acknowledged.

Appendix A. Supplementary data

Supplementary data to this article can be found online at https://doi.org/10.1016/j.ejmech.2019.02.078.

References

[1] T. Mena-Barragán, M.I. García-Moreno, A. Sevšek, T. Okazaki, E. Nanba, K. Higaki, N.I. Martin, R.J. Pieters, J.M. García Fernández, C. Ortiz Mellet, Probing the inhibitor versus chaperone properties of sp2-Iminosugars towards human β-glucocerebrosidase: a picomolar chaperone for Gaucher disease, Molecules 23 (2018) 927.

[2] T. Mena-Barragán, M.I. García-Moreno, E. Nanba, K. Higaki, A.L. Concia, P. Clapés, J.M. García Fernández, C. Ortiz Mellet, Inhibitor versus chaperone behaviour of D-fagomine, DAB and LAB sp^2-iminosugar conjugates against glycosidases: a structure-activity relationship study in Gaucher fibroblasts, Eur. J. Med. Chem. 121 (2016) 880–891.

[3] A. de la Fuente, R. Rísquez-Cuadro, X. Verdaguer, J.M. García Fernández, E. Nanba, K. Higaki, C. Ortiz Mellet, A. Riera A, Efficient stereoselective synthesis of 2-acetamido-1,2- dideoxyallonojirimycin (DAJNAc) and sp^2-iminosugar conjugates: novel hexosaminidase inhibitors with discrimination capabilities between the mature and precursor forms of the enzyme, Eur. J. Med. Chem. 121 (2016) 926–938.

[4] E.M. Sánchez-Fernández, R. Rísquez-Cuadro, M. Aguilar-Moncayo, M.I. García-Moreno, C. Ortiz Mellet, J.M. García Fernández, Generalized anomeric effect in *gem*-diamines: stereoselective synthesis of α-*N*-linked disaccharide mimics, Org. Lett. 11 (2009) 3306–3308.

[5] E.M. Sánchez-Fernández, J.M. García Fernández, C. Ortiz Mellet, Glycomimetic-based pharmacological chaperones for lysosomal storage disorders: lessons from Gaucher, GM1-gangliosidosis and Fabry diseases, Chem. Commun. 52 (2016) 5497–5515.

[6] M.I. García-Moreno, F. Ortega-Caballero, R. Rísquez-Cuadro, C. Ortiz Mellet, J.M. García Fernández, The Impact of heteromultivalency in lectin recognition and glycosidase inhibition: an integrated mechanistic study, Chem. Eur J. 23 (2017) 6295–6304.

[7] E.M. Sánchez-Fernández, C.D. Navo, N. Martínez-Sáez, R. Goncalves-Pereira, V.J. Somovilla, A. Avenoza A, J.H. Busto, G.J.L. Bernardes, G. Jiménez-Osés, F. Corzana, J.M. García Fernández, C. Ortiz Mellet, J.M. Peregrina, Tn Antigen mimics based on sp^2-iminosugars with affinity for an anti-MUC1 antibody, Org. Lett. 18 (2016) 3890–3893.

[8] V.F. Vartabedian, P.B. Savage, L. Teyton, The processing and presentation of lipids and glycolipids to the immune system, Immunol. Rev. 272 (2016) 109–119.

[9] E.M. Sánchez-Fernández, R. Rísquez-Cuadro, M. Chasseraud, A. Ahidouch, C. Ortiz Mellet, H. Ouadid-Ahidouch, J.M. García Fernández, Synthesis of *N*-, *S*-, and *C*-glycoside castanospermine analogues with selective neutral α-glucosidase inhibitory activity as antitumor agents, Chem. Commun. 46 (2010) 5328–5330.

[10] G. Allan, H. Qualid-Ahidouch, E.M. Sánchez-Fernández, R. Rísquez-Cuadro, J.M. García Fernández, C. Ortiz Mellet, A. Ahidouch, New castanospermine glycoside analogues inhibit breast cancer cell proliferation and induce apoptosis without affecting normal cells, PLoS One 8 (2013) e76411.

[11] N. Gueder, G. Allan, M.S. Telliez, F. Hague, J.M. García Fernández, E.M. Sánchez-Fernández, C. Ortiz Mellet, A. Ahidouch, H. Ouadid-Ahidouch, sp^2-Iminosugar α-glucosidase inhibitor 1-*C*-octyl-2-oxa-3-oxocastanospermine specifically affected breast cancer cell migration through Stim1, beta1-integrin, and FAK signaling pathways, J. Cell. Physiol. 232 (2017) 3631–3640.

[12] E.M. Sánchez-Fernández, V. Gómez-Pérez, R. García-Hernández, J.M. García Fernandez, G.B. Plata, J.M. Padrón, C. Ortiz Mellet, S. Castanys, F. Gamarro, Antileishmanial activity of sp^2-iminosugar derivatives, RSC Adv. 5 (2015) 21812–21822.

[13] A.I. Arroba, E. Alcalde-Estévez, M. García-Ramírez, D. Cazzoni, P. de la Villa, E.M. Sánchez-Fernández, C. Ortiz Mellet, J.M. García Fernández, C. Hernández, R. Simó, A.M. Valverde, Modulation of microglia polarization dynamics during diabetic retinopathy in *db/db* mice, Biochim. Biophys. Acta 1862 (2016) 1663–1674.

[14] E. Alcalde-Estévez, A.I. Arroba, E.M. Sánchez-Fernández, C. Ortiz Mellet, J.M. García Fernández, L. Masgrau, A.M. Valverde, The sp^2-iminosugar glycolipid 1-dodecylsulfonyl-5*N*,6*O*-oxomethylidenenojirimycin (DSO_2-ONJ) as selective anti-inflammatory agent by modulation of hemeoxygenase-1 in Bv.2 microglial cells and retinal explants, Food Chem. Toxicol. 111 (2018) 454–466.

[15] P. Bogdanov, L. Corraliza, J.A. Villena, A.R. Carvalho, J. García-Arumi, D. Ramos, J. Ruberte, R. Simó, C. Hernández, The *db/db* mouse: a useful model for the study of diabetic retinal neurodegeneration, PLoS One 9 (2014) e97302.

[16] E.M. Sánchez-Fernández, R. Gonçalves-Pereira, R. Rísquez Cuadro, G.B. Plata, J.M. Padrón, J.M. García Fernández, C. Ortiz Mellet, Influence of the configurational pattern of sp^2-iminosugar pseudo *N*-, *S*-, *O*- and *C*-glycosides on their glycoside inhibitory and antitumor properties, Carbohydr. Res. 429 (2016) 113–122.

[17] D. Bell, J.W. Young, J. Banchereau, Dendritic cells, Adv. Immunol. 72 (1999) 255–324.

[18] R.L. Danner, R.J. Elin, J.M. Hosseini, R.A. Wesley, J.M. Reilly, J.E. Parillo, Endotoxemia in human septic shock, Chest 99 (1991) 169–175.

[19] M. Kobayashi, S. Saitoh, N. Tanimura, K. Takahashi, K. Kawasaki, M. Nishijima, Y. Fujimoto, K. Fukase, S. Akashi-Takamura, K. Miyake, Regulatory roles for MD-2 and TLR-4 in ligand-induced receptor clustering, J. Immunol. 176 (2006) 6211–6218.

[20] W.Y.C. Lu, C. Yeh, P.S. Ohashi, LPS/TLR-4 signal transduction pathway, Cytokine 42 (2008) 145–151.

[21] F. Peri, V. Calabrese, Toll-like receptor 4 (TLR-4) modulation by synthetic and natural compounds: an update, J. Med. Chem. 57 (2014) 3612–3622.

[22] V. Flacher, P. Neuberg, F. Point, F. Daubeuf, Q. Muller, D. Sigwalt, J.D. Fauny, J.S. Remy, N. Frossard, A. Wagner, C.G. Mueller, E. Schaeffer, Mannoside glycolipid conjugates display anti-inflammatory activity by inhibition of Toll-like receptor-4 mediated cell activation, ACS Chem. Biol. 10 (2015) 2697–2705.

[23] L. Dehuyser, E. Schaeffer, O. Chaloin, C.G. Mueller, R. Baati, A. Wagner, Synthesis of novel mannoside glycolipid conjugates for inhibition of HIV-1 transinfection, Bioconjug. Chem. 23 (2012) 1731–1739.

[24] E. Schaeffer, L. Dehuyser, D. Sigwalt, V. Flacher, S. Bernacchi, O. Chaloin, J.S. Remy, C.G. Mueller, R. Baati, A. Wagner, Dynamic micelles of mannoside glycolipids are more efficient than polymers for inhibiting HIV-1 transinfection, Bioconjug. Chem. 24 (2013) 1813–1823.

[25] J.J. Gills, S.S. Castillo, C. Zhang, P.A. Petukhov, R.M. Memmott, M. Hollingshead, N. Warfel, J. Han, A.P. Kozikowski, P.A. Dennis, Phosphatidylinositol ether lipid analogues that inhibit AKT also independently activate the stress kinase, p38alpha, through MKK3/6-independent and -dependent mechanisms, J. Biol. Chem. 282 (2007) 27020–27029.

[26] C.A. Sanhueza, A.C. Arias, R.L. Dorta, J.T. Vázquez, Absolute configuration of glycosyl sulfoxides, Tetrahedron: Asymmetry 21 (2010) 1830–1832.

[27] N. Khiar, Determination of the absolute configuration of sulfinyl glycosides: the role of the *exo*-anomeric effect, Tetrahedron Lett. 41 (2000) 9059–9063.

[28] C. Aerts-Toegaert, C. Heirman, S. Tuyaerts, J. Corthals, J.L. Aerts, A. Bonehill, K. Thielemans, K. Breckpot, CD83 expression on dendritic cells and T cells: correlation with effective immune responses, Eur. J. Immunol. 37 (2007) 686–695.

[29] J.-G. Li, Y.-M. Du, Z.-D. Yan, J. Yan, Y.-X. Zhuansun, R. Chen, W. Zhang, S.-L. Feng, P.-X. Ran, CD80 and CD86 knockdown in dendritic cells regulates Th1/Th2 cytokine production in asthmatic mice, Exp. Ther. Med. 11 (2016) 878–884.

[30] T.A. Ignatowski, S. Gallant, R.N. Spengler, Temporal regulation by adrenergic receptor of macrophage (Mϕ)-derived tumor necrosis factor (TNF) production post-LPS challenge stimulation, J. Neuroimmunol. 65 (1996) 107–117.

[31] D.L. Horton, D.G. Remick, Delayed addition of glucocorticoids selectively suppresses cytokine production in stimulated human whole blood, Vaccine Immunol 17 (2010) 979–985.

[32] M.A. Erickson, W.A. Banks, Cytokine and chemokine responses in serum and brain after single and repeated injections of lipopolysaccharide: multiplex quantification with path analysis, Brain Behav. Immun. 25 (2011) 1637–1648.

[33] S. Copeland, H.S. Warren, S.F. Lowry, S.E. Calvano, D. Remick, Acute inflammatory response to endotoxin in mice and humans, Clin. Diagn. Lab. Immunol. 12 (2005) 60–67.

[34] M.C. Bryan, N.S. Rajapaksa, Kinase inhibitors for the treatment of immunological disorders: recent advances, J. Med. Chem. 61 (2018) 9030–9058.

[35] T. Sterling, J.J. Irwin, ZINC 15 – Ligand discovery for everyone, J. Chem. Inf. Model. 55 (2015) 2324–2337.

[36] P. Díaz-Pérez, M.I. García-Moreno, C. Ortiz Mellet, J.M. García Fernández, Synthesis and comparative glycosidase inhibitory properties of reducing castanospermine analogues, Eur. J. Org. Chem. (2005) 2903–2913.